International Journal of Power Electronics and Drive System (IJPEDS)
Vol. 17, No. 4, December 2026, pp. 2413~2426
ISSN: 2088-8694, DOI: 10.11591/ijpeds.v17.i4.pp2413-2426

Impact of air gap on the operational characteristics of linear induction motors

Ahmed Saad Yahya[1], Abdullah K. Shanshal[2], Ahmed Hasim Ahmed[3], Ahmed Jadaan Ali[1], Basil Mohammed Saied[4], Tamer Kamel[5]
[1]Department of Electrical Techniques Engineering, Engineering Technical College Mosul, Northern Technical University, Mosul, Iraq
[2]Department of Unmanned Aerial Vehicles Engineering Techniques, Engineering Technical College Mosul, Northern Technical University, Mosul, Iraq
[3]Department of Computer Techniques Engineering, Technical Engineering, College for Computer and Artificial Intelligence, Northern Technical University, Mosul, Iraq
[4]Department of Electrical Engineering, College of Engineering, University of Mosul, Mosul, Iraq
[5]School of Engineering, Computing and Mathematics, University of Plymouth, Plymouth, United Kingdom

Article Info

Article history:

Received Jan 20, 2026
Revised Aug 25, 2026
Accepted Sep 13, 2026

Keywords:

Finite element method
Linear induction motor
Magnetic air gap flux density
Motor efficiency
Thrust force

ABSTRACT

Electric machines are considered one of the most important tools, which can be utilized for different applications including electric vehicles, robots, domestic appliances, as well as transportation. Nowadays, induction machines have extinguished merits make it a contender among other machines. More specifically, linear induction motors (LIM) have gained popularity compared with other non-conventional applications due to high efficiency and reliability, high torque, and low vibration, which specify it to be used in different areas such as high rail-speed transport. In addition, forces produced at (LIMs) are relatively high and can be used where intensive power density is required along with the minimum occupied area. This work revolves around the analysis of the operational characteristics of the three-phase linear induction motor using the finite element modeling method. More specifically, the analysis of the thrust, speed, power factor, and flux density is investigated. Besides that, the effect of varying the air gap on motor efficiency, with special emphasis on the power factor improvement, is presented. Consequently, air gap length variation from 30 mm to 5 mm was found to improve the predicted thrust force by about 15-35%, depending on operating speed, providing a numerical basis for air-gap selection.

This is an open access article under the CC BY-SA license.

Corresponding Author:

Ahmed Jadaan Ali
Department of Electrical Techniques Engineering, Engineering Technical College Mosul
Northern Technical University
Mosul, Iraq
Email: ahmed.j.ali@ntu.edu.iq

1. INTRODUCTION

Linear induction motors (LIMs) are electrical-driven tool that create straight movement instead of the rotary movement of conventional motors. These are ideal for many applications such as transportation systems, conveyors, and actuators [1], [2]. It has no rotary to linear conversion mechanisms incorporated in its structure and design as in the case of rotary cars; thus, layout complexity and maintenance costs are lower. Therefore, LIMs are mainly positive in the places that call for direct linear movement, including maglev trains, automatic part production processes, and airport baggage handling shelved systems [3]. The main part of the LIM is a layered sheet of iron-containing three-phase windings, while the second part is a solid iron core combined with a conductor material, aluminum or copper, arranged along the length of the machine.

However, discrete representation of LIMs machines has a crucial role in increasing general performance and dependability, particularly when modeling the three-phase linear motor using conventional methods such as the DQ model or the three-phase dynamic model. On the other hand, establishing several physical interactions of the machine has become possible by using more elaborate methods [4], [5]. In this paper, the leading parameters of LIMs, including their typical dimensions such as length, width and height as well as air-gap parameters are identified as one of the key subjects that must be addressed with high accuracy, since an improperly selected air gap directly compromises the machine's efficiency, thrust and steadiness of operation.

Therefore, it is ascertained that under normal and especially abnormal conditions of such machines, the finite element method (FEM) is more suitable to describe the electromagnetic characteristics [6]-[9]. Prior relevant research focused on the effect of the air gap in three-phase LIMs, in general, focusing on the assessment of both the electrical and mechanical characteristics. The intermediate space between the stator and the mover controls certain parameters such as current, force, and mechanical forces [10]-[12]. The effect of the air-gap dimensions and parameters and the magneto motive force are also proportional to the motor design as well as the operational frequency. On the other hand, when the air gap increases electrical losses increase within the peripheral motor due to eddy current losses and magnetic leakages and reduces the thrust available. Furthermore, a larger air gap means that the generated magnetic field and the force applied across the surface of the motor will not be uniform, resulting irregular movement and affect the steadiness of the motor's performance. To minimize such impacts, there has been an effort both in the design of new coils configuration and the application of superior magnetic materials for handling the increased air gap [12]-[16]. It is worth noting that these prior studies differ in emphasis: references [10]-[12] quantify the electrical loss mechanisms associated with the intermediate air gap without directly reporting the corresponding thrust-force trend, whereas references [12]-[16] focus on mitigating the effect of an enlarged air gap through coil and material redesign rather than quantifying the air-gap dependence itself; the present work addresses this gap by jointly and systematically quantifying both the thrust-force and efficiency trends across a range of operating speeds.

Despite this substantial volume of work, most of the studies that have been done focus on either a qualitative, or a single fixed operating speed, study, and rarely test their finite element predictions with another analytical model. However, designers are still lacking of a systematic, validated framework to quantify the combined performance and mechanical system response to the air-gap length over a range of operating speeds, information that is essential for selecting the air-gap length which is optimal for a specific trade-off between performance and mechanical constraints. In this research paper, a comprehensive mathematical model using the FEM for predicting the operational characteristics of the proposed LIMs is presented, and the predicted results are verified through comparison with the analytical work of the previously approved study. The approach used for the research methodology ensures minimization of computational effort with more efficiency and accuracy of results. It is especially useful in this context, as it allows the study of the effects of the variation in air gap length on the indicators of the machine's performance. In addition, the mapping strategy used in this paper provides a significant alleviation of the time and workforce needed to solve intricate computational problems. Therefore, it provides a success in emphasizing the model sensitivity by accurately implementing the machine's physical appearance and incorporating electromagnetic conditions into the simulation process to quantify their impacts. In addition, simulation integrates the boundary conditions of the proposed model and considers the mechanical coupling effect on the motor primordial components [17]-[19]. The slip factor of the motor, which is defined as the difference between the synchronous speed of the motor and its actual operating speed, can also be determined easily once the motor is in operation [20]. In this paper, the correlation between oscillation in the air gap and the motor efficiency is determined, with emphasis on evaluating the effect of this fluctuation on the performance of the motor. In particular, this work has developed in ANSYS Maxwell a combined analytical-numerical model which, to the authors' knowledge, has not been reported in previous studies of LIM air-gap systems, where the effect of the air-gap length (5-30 mm) on the thrust force and efficiency has been systematically quantified and validated, for this activity; i) the analytical derivation of the magnetic motive force (MMF) and electromagnetic field equations for the machine, ii) the validation of FEM predictions against such analytical equations, and iii) the systematic quantification of the effect of the air-gap length (5-30 mm) on the thrust force and efficiency across three operating speeds. The investigated air-gap range (5-30 mm) and the three operating speeds were selected to bracket the mechanical clearances and travel speeds typically reported for practical LIM installations such as maglev and rail-based transport, so that the study’s quantitative guidance remains directly applicable to real design constraints.

Beyond the electromagnetic design of the machine itself, the quantified thrust-efficiency-air-gap relationship developed in this study is also directly relevant to the power-electronics side of LIM drive systems. More specifically, it can inform the current and voltage ratings required of the traction converter for a given expected air-gap tolerance, motivate closed-loop control strategies that compensate for air-gap drift (e.g., adaptive slip-frequency or thrust-force regulation in response to a measured or estimated change in air gap). Furthermore, it can support the design of electric-drive systems for renewable-energy-linked applications such

as linear generators used in wave and tidal energy converters. Such LIM-based transportation, handling, or energy-conversion systems are connected to a wider electrical network, the predictable, quantified efficiency behavior reported in this work can also support their integration into smart-grid-aware load and energy management schemes.

2. MMF ANALYSIS OF LINEAR INDUCTION MOTORS (LIMs)

The study focused on the research design and approach topics. In this study, a methodology was used, which consisted of an analytical electromagnetic formulation of the LIM and a numerical simulation using the FEM performed in the computer software ANSYS Maxwell. It was decided to adopt this hybrid (analytical-numerical) design because the analytical MMF and field equations (The operational characteristics of each motor are calculated and compared against (1)-(16) for thrust force, speed, current and efficiency, respectively, and validated with the FEM results, while the non-linear material behavior, discrete winding geometry, and air-gap effects are captured by the FEM model, which these analytical equations cannot resolve. Therefore, such a combination is suitable for systematically studying the effect of the variation of air-gap length on the performance of the proposed LIM, filling the gap identified in section 1, which is the absence of a validated relationship between air-gap length and thrust force and efficiency for different operating speeds. Models/algorithms/techniques. The mathematical model of the proposed LIM is settled in two steps: First, the mathematical model of the machine is derived in the form of analytical MMF and winding-distribution model (1)-(7), and second, the governing electromagnetic field equations (Maxwell's equations, magnetic vector potential formulation, and the Laplace/Poisson equations. The following (8)-(18) are numerically solved using FEM. The set of these equations, along with Figures 1-3, forms the full analytical-numerical prediction model and algorithmic procedure for the operational properties of the machine. In general, the MMF is considered the basis for the operation of motors, as this force is responsible for generating the magnetic field in the motor. The magnetic driving force is produced by the passage of current through the motor coils, which in turn produces a flowing magnetic field that interacts with the secondary part of the motor. Meanwhile, when a three-phase alternating current source is applied to the motor coils, currents are generated, producing variable magnetic fields over a period of time. Due to the phase difference between these three phases (120 degrees in each coil), the waves of electromotive force are produced that change in value with time and are transmitted along the stator of the motor [21]. The effect of the traveling wave of magneto motive force is developed by summing up the MMFs generated from the respective three-phase windings, which are distributed through the length of LIMs. The generated MMF wave is crucial for the motor operation because it brings currents into the secondary part (the conductive plate) with a thrust force that pushes the secondary part of the proposed model.

The velocity of the traveling MMF wave (Vm) can be expressed as [7], [22]:

$$Vm = (2 * f * t)/p \quad (1)$$

where (τ)is the pole pitch, (f) is the frequency of the applied source to the motor, and (P) is the number of pole pairs of the proposed model. As a sequences, the transferring the magnetic field generated in the primary part to the secondary part results in the passage of an eddy current in the secondary conductor, the generated eddy currents produce a magnetic field opposite to the main magnetic field generated in the primary, and this difference generates a force that pushes the secondary part forward and thus generates the linear movement of the motor [23], [24]. Consequently, the magnetic motive force MMF is distributed along the length of the linear motor, forming a sinusoidal shape and changing in value with time. However, this distribution is irregular in the linear motor but important in generating the thrust resulting from the motor and its efficiency as well. The distribution of the magnetic motive force depends on several factors including the way the motor coils are wound, the shape of the current wave, as well as the design of the magnetic circuit [25], [26]. Analytically, it is possible to analyze the distribution of the MMF using the Fourier series theory, which divides the wave into a number of harmonics consisting of the fundamental harmonic responsible for the operation of the motor and other harmonics that lead to undesirable effects on the performance of the motor through running case, such as acoustic noise and vibrations [15], [27]. This section of the research explains how the motor coils are distributed, how these coils are wound, and how MMF is generated in the three-phase linear motors (LIMs) and transmitted to the secondary part, resulting in a mobile magnetic field responsible for operating the motor [28]. The process of arranging and distributing the coils within the stator geometry is important because these coils produce the magnetic field necessary to move the motor, which in turn affects the shape of the generated MMF and the generated harmonics [29], [30]. The arrangement of coils consists of a single layer of coils, or the coil consists of two layers within the slots of the stator [31]. The windings of each phase are spaced 120 electrical degrees apart from each other to create a balanced three-phase system.



Figure 1. Double-layer stator winding configuration

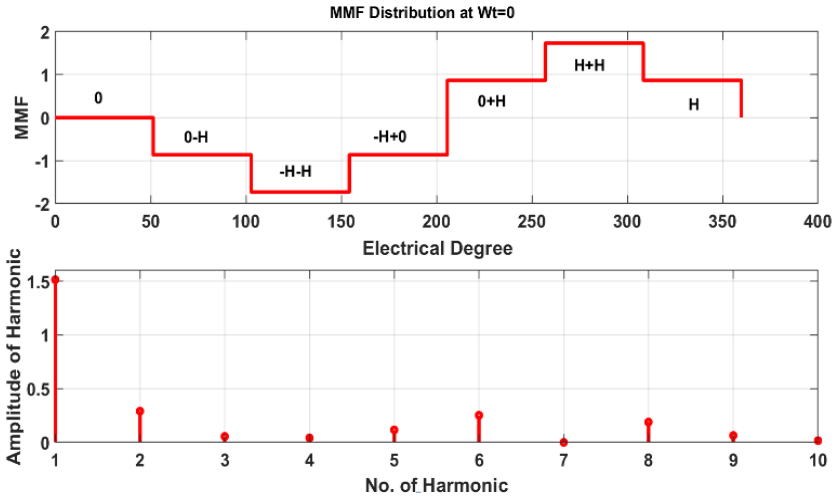

Figure 2. MMF distribution of the proposed LIM model

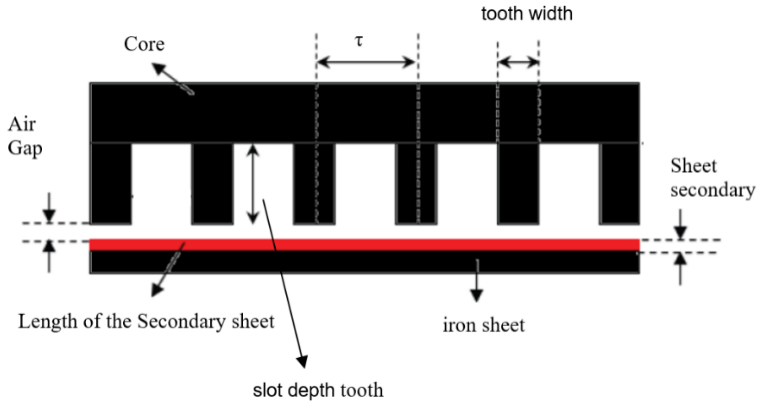

Figure 3. Geometric shape of the LIM

Figure 1 indicates the configuration of the double-layer winding with two poles for the proposed model. This configuration improves the roundness of the MMF, decreases the harmonic distortion, and, in turn, increases motor efficiency. Moreover, the double-layer winding configuration reduces the effect of the clogging forces that cause violent vibration and noise, making operations smoother. Moreover, the value of the slot angle has an important effect on the motor's behavior and harmonics in the motor [17], [32].

Slot angle = (360×2)/number of slots per pole (2)

For (7 slots per pole), the slot angle is = 102.86 electrical degrees. In addition, the pole pitch (τ) refers to the distance, in terms of slots, between the centers of two adjacent poles. It is a key parameter in coil design, as it helps determine the spacing between coils and the assignment of slots to optimize performance. The formula for calculating the pole pitch is:

Pole pitch (τ) =Total number of slots/number of poles (3)

The value of the pole pitch for the same number of slots (7 slots per pole and the number of poles (2 poles), is: (τ = 3.5 slots per pole). This implies that each pole measures 3.5 slots; this value is very important

and should be precisely calculated and considered in designing the winding pattern and returning a near-balanced magnetic field in the motor. The expression of the mechanical angle per slot, as well as the pole angle, are expressed as shown in (2) and (3), respectively.

$$\text{Mechanical angle per slot} = 360/\text{total number of slots} = 51.43 \quad (4)$$

Where the pole angle can be calculated as: Pole Angle = Mechanical Angle per Slot × Pole Pitch = 51.43×3. 5 = 180. Which are equal for the proposed model (51.43 & 180°) respectively. On the other hand, it is possible to represent the motor's MMF wave at any instant. For example, the MMF vector can be situated at ωt = 0, as shown in Figure 2.

To calculate the magnetic motive force (MMF), the relationship between the current and the number of turns in the coil or coils generating the magnetic field is used. Magnetomotive force is a measure of the ability of an electric current passing through a coil to generate a magnetic field. The general formula for calculating the magnetomotive force is: (MMF=N*I), where: N is the number of turns in the coil, I is the current passing through the windings (in amperes). For concentric winding within the slots and the resulting generated current per turn, the equation of the three-phase currents for the proposed model can be expressed as (5)-(7).

$$I_A = K \sin(wt) = 0 \quad (5)$$

$$I_B = K \sin(wt - 2pi/3) = - 0.866\ K = -H \quad (6)$$

$$I_C = K \sin(wt+2pi/3) = 0.866\ K = H \quad (7)$$

For ideal machines, the shape of the generated MMF is like a sine wave with fewer harmonics. However, experimentally, the distribution of windings is not perfectly uniform, and the current is not equally distributed, hence, the MMF is not measured perfectly or precisely due to the variation in the air gap between the stator and the rotation part which causes messing up the MMF wave. Consequently, there will be additional harmonics that appear to distort the waveform. These space harmonics are sinusoidal waves with frequencies that are integer multiples of their fundamental frequency. Mathematically, the frequencies of these harmonics are written in terms of multiples of (2pi/ τ), where (τ) refers to motor pole pitch [33].

3. PROPOSED PARAMETERS OF LIM

The FEM presents a great and informative method for electrical and technical evaluation of LIM's performance and parameters. By decomposing the motor into several segments, which are easier for an FEM tool to solve, one can model the motor based on the electromagnetic fields, as well as the electrical and mechanical currents and forces, respectively. Resulting a clear picture of the stator and the secondary part such as the conductive plate to capture the interaction needed for analyzing the output characteristics of the machines such as thrust force, torque, and efficiency [34], [35]. Moreover, FEM simulates the distribution of the magnetic flux density and current in the motor as influenced by the air gap dimensions, positions, and type of the windings, as well as the properties of the machine material. More specifically, the dimension of the air gap parameter in the motor has a notable impact on the performance of the motor. It is found that the variation of the air gap influences the magnetic field flux, which in turn affects the global efficiency and thrust. This can be precisely predicted and investigated by using FEM and serves to calculate eddy current losses, magnetic leakage as well as other forms of power loss which may reduce efficiency [36], [37]. Apart from electromagnetic analysis, FEM can also be used to predict the thermal loads that take place in motors, and hence it will be useful in estimating the temperature of the motor and preventing the generation of heat beyond the limits of the motor. In addition, reliability analysis using FEM enables the assessment of response characteristics under different operating conditions such as loads and transients in order to meet the optimum design for the LIM, which is more efficient, better performing, and more reliable in various and actual power applications [38].

A three-phase LIM is characterized by a rectangular geometry that consists of two primary components: namely the stator and the secondary part. The stator consists of laminated iron cores with three-phase windings for construction and functions to create a traveling magnetic field when energized. This component is rectangular and has a length equal to the length of the motor; the cross-section of this part should be as optimized as possible to achieve an even distribution of magnetic flux as well as efficient coil placement. The second part, which can also be created using aluminum or copper (commonly followed by a solid iron core), is installed to be parallel to the stator. To increase the coupling between the plates, this plate. The size of the LIM, normally defined as the length, width, and available height, depends on specific application needs including thrust force, speed, and load. These geometrical characteristics, combined with FEM analysis to give adequate insight into the motor's behavior, make it a contender for particular industrial applications. Table 1 gives the specific design dimensions

of the proposed LIM used in the simulation, which forms the basis for further FEM analysis and performance assessment [39]. Table 1 illustrates the parameters of the proposed LIM (3.75 kW, 380 V, 3-phase, 7 stator slots, and 2 poles) used in the FEM model simulation of this work [39], [40].

Table 1. Data of LIM used in the simulation [40]

Parameter	Value	Parameter	Value
Phase number	3	Primary height	58 mm
No. Of poles	2	Air gap	15 mm
Frequency	50 HZ	Length of the secondary sheet	6 m
Rated voltage	380 V	Secondary sheet thickness	5 mm
Rated output power	3.75 Kw	Number of turns per phase	300
Number of stator slots	7	Coil resistance	12.56 ohm
Length of the primary core	270 mm	Inductance	169.6 mH
Tooth width	25.25 mm	Hs2	37 mm
Tooth height	37	Bs0	6.5 mm
Slot width	13 mm	Bs1	13 mm
Hs0	0	Bs2	13 mm

4. MODELING OF LIMs USING FEM

Based on FEM, the geometrical modeling and characteristics investigation of the linear induction machines offers comprehensive and accurate analysis as well as enhanced performance and reliability. The process has several critical stages required to obtain an accurate representation and analysis of the data collected. First, an elaborated geometrical model of the LIM is created, including stator, mover, slots, and winding configurations. This geometry is then meshed into smaller parts for 2D triangles or quadrilaterals and 3D tetrahedral or hexahedral elements. For the LIM material, the magnetic permeability and conductivity of each element are determined and set to represent the physical characteristics of the materials accurately. Constraints are then set, which include the values of voltage or current input and any externally controllable factors such as temperature or weather conditions, as well as boundary conditions. Employing the fundamentals of electromagnetics, the behavior of the Lorentz force induction motor is described by the appropriate equations such as Maxwell equations, together for circuits and motion where necessary is also incorporated. These equations are discretized and numerically solved iteratively by FEM to compute electromagnetic field distribution, air gap flux density, current, and forces inside the LIM. As a third alternative, a transient analysis can be performed to examine the LIM dynamic performance under different working conditions, such as starting and breaking. Meanwhile, the extension of these equations for quasi-static fields can be considered as more general extensions of these fundamental principles that enrich the analysis framework [18], [40]. The relative motion between the primary and secondary parts was simulated by the band (moving-mesh) technique in the FEM model implemented and solved with the transient 2-D solver in ANSYS Maxwell's.

4.1. Mesh and solver settings

The computational domain was discretized using an adaptive triangular mesh, locally refined in the air-gap region and along the secondary-plate surface where the eddy-current and leakage-flux gradients are highest. Mesh density was increased in successive refinement steps until the predicted thrust force no longer changed appreciably between refinements, confirming that the reported results are independent of the mesh resolution. The transient 2-D solver was run over multiple successive electrical cycles with a time step sized to resolve the fundamental MMF waveform, and the solution was accepted once the field quantities reached a steady, cycle-to-cycle repeating state, indicating numerical convergence. A zero magnetic vector potential (Dirichlet condition, $A = 0$) was imposed on the outer boundary of the simulation domain, placed a sufficient distance from the stator back-iron to avoid artificially constraining the field; continuity of the tangential field components was enforced across all internal material interfaces, and the relative motion of the secondary plate was represented through the band (moving-mesh) technique.

4.2. Validation/evaluation strategy

The accuracy of the developed FEM model has been tested by comparing the simulation results of the speed, thrust force, and the current waveforms with the results of the analytical MMF and the electromagnetic equations given in the equations. Prior to using the FEM model for the air-gap sensitivity study, a good correlation was reported between the two approaches (see Section 5), which verifies the validity of the FEM model. Quantitatively, the FEM-predicted thrust force, speed, and current waveforms tracked the corresponding analytical MMF-based predictions closely and consistently across the operating range covered by (1)-(18), with the discrepancy remaining within the few-percent tolerance band typically reported for FEM-

versus-analytical validation of comparably sized LIMs, which is considered acceptable engineering accuracy and further supports the validity of the FEM model used for the subsequent air-gap sensitivity study.

4.3. Ethical considerations

In this study, the motor used is a linear induction motor, and the study is purely analytical and numerical simulation using finite element analysis.

$$\nabla \times H = J \tag{8}$$

$$\nabla \times E = -\frac{dB}{dt} \nabla . B = 0 \tag{9}$$

$$J = \sigma . E, B = \mu . H \tag{10}$$

Where: J is the current density (Amp/m^2). H is the magnetic field intensity (A/m). B is the magnetic flux density (web/m2). E is the electric field strength (volt/m). t is the time (sec). σ is the conductivity of the cloth (Ω.m), and μ is the magnetic permeability coefficient of the fabric (H/m). The family members in (2) and (3) represent the constituent equations; they are utilized collectively with Maxwell's equations, as well as explain the interactions among the subject amounts established totally on the magnetic and electric-powered houses of materials μ and σ. The provided content discusses Maxwell's equations and their application in electromagnetism, particularly in relation to the magnetic vector potential (MVP). Here's a breakdown of the key points [10], [41]-[43].

$$B = \nabla \times A \tag{11}$$

Substituting (2) and (3) into (4) gives:

$$\nabla \times (\frac{1}{\mu \nabla \times A}) = J \tag{12}$$

with $\nabla \times (\nabla \times A) = \nabla . (\nabla . A) - \nabla^2 A$ and $\nabla . (\nabla . A)$ = zero, (5) turns into:

$$\nabla^2 A = -\mu . J \tag{13}$$

Maxwell's calculations applied in electric motors are categorized into two parts, that is Laplace's (11) and Poisson's (10). The first kind of equation describes the electromagnetic subject circulation inside the middle and air-gap areas. The second one is used to indicate the field constraints in the stator coil and the strong movable metal plate [42].

$$\nabla^2 A = zero \tag{14}$$

Based on Faraday, regulation and replacing the attractive vector capability A and electric scalar capability V in (2) can be represented as:

$$E = -(dA/dt + \nabla V) \tag{15}$$

Then, substituting (10) into (9) determines the cutting-edge density [44].

$$J = \sigma . E = -\sigma(dA/dt + \nabla V), J = Js + Jb + Jd \tag{16}$$

Where Js is the voltage source current concentration, Jb is the eddy current concentration, and Jd is the movement mode concentration. The linear pace of the motor can be given using [19], [27]:

$$Vs = (2 * f * t)/p \text{ M/sec} \tag{17}$$

$$V = (1 - s)Vs \text{ M/sec} \tag{18}$$

where Vs is the synchronous velocity of the linear traveling field. t is the width pole pitch; f is the supply frequency; v is the velocity of the linear traveling motor; and s is the slip factor of the motor.

5. CALCULATIONS AND RESULTS

In this research, the proposed LIM motor with 2-pole/7-slot is characterized during steady-state operation by measuring the speed of (48.5 km/h) (about 128.6 r.p.m.) and the air gap of (15) mm between the

primary and the secondary side of the motor. This particular configuration provides the best efficiency and is essential to achieve the correct analysis of the electromagnetic and mechanical characteristics of the motor. Figure 4 illustrates the possibility of operating the motor at an efficiency level not achievable in traditional stationary setups, sufficient thrust output, and the dynamic response of the system under real-world conditions.

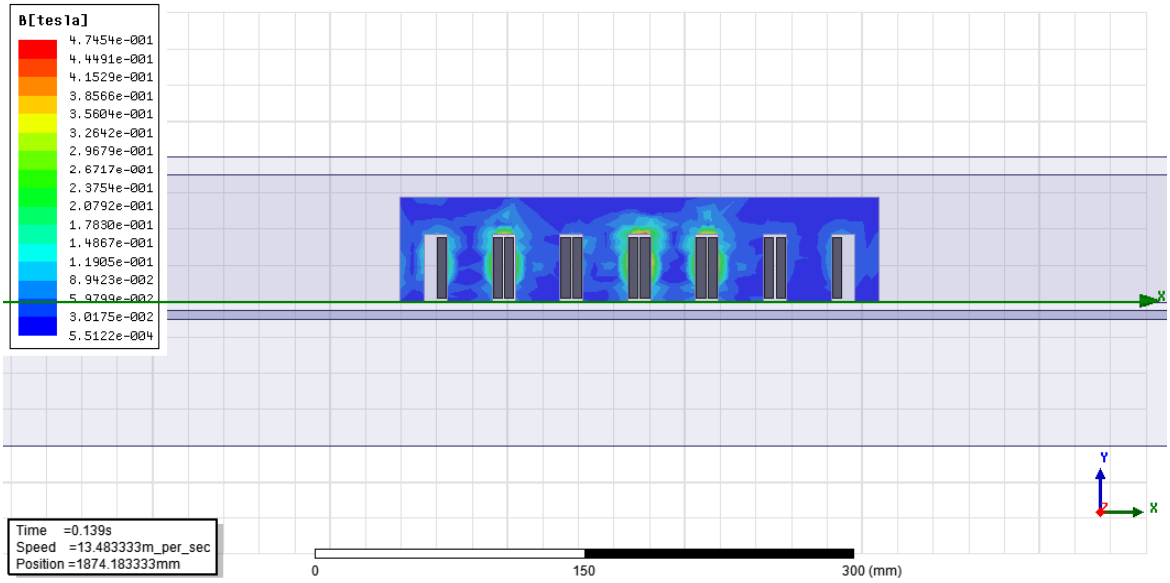

Figure 4. Magnetic flux density for LIM (FEM-model)

The dimensions of the proposed model are shown in Table 1, and its brief specifications are listed in Table 2. Figure 5 shows speed operation under normal condition configuration of the proposed LIM model. Figure 6 shows the phase current of the machine; it is noted that there is an imbalance in the values of the three-phase currents, and this is due to the arrangement of the coils designed for this machine, as their ends are irregular. Moreover, the engine performance is investigated and analyzed by changing the value of the air gap length between the metal plate and the moving part to find its effect on the engine efficiency. Different cases of the air gap value are considered, and the efficiency of the linear motor is calculated at different speeds, as shown in Figure 7.

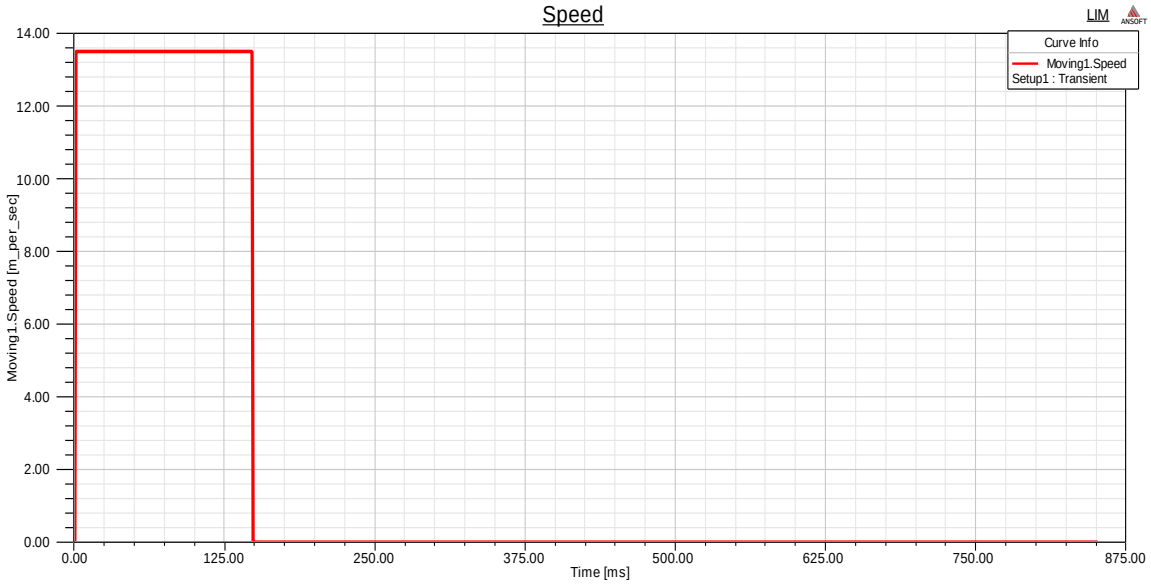

Figure 5. Speed (velocity) for LIM

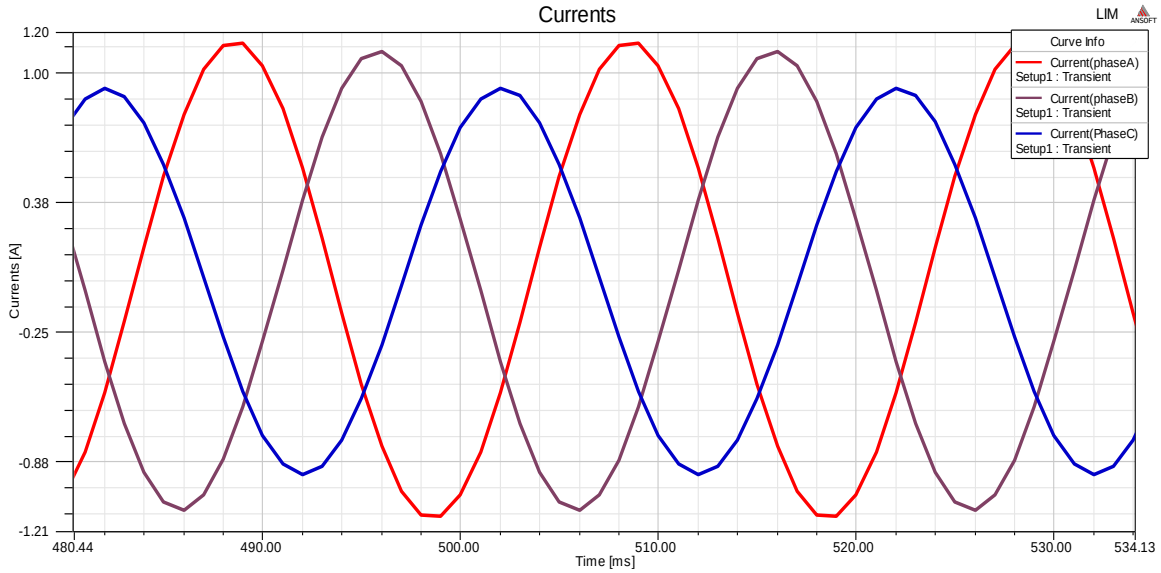

Figure 6. Three phase currents for LIM

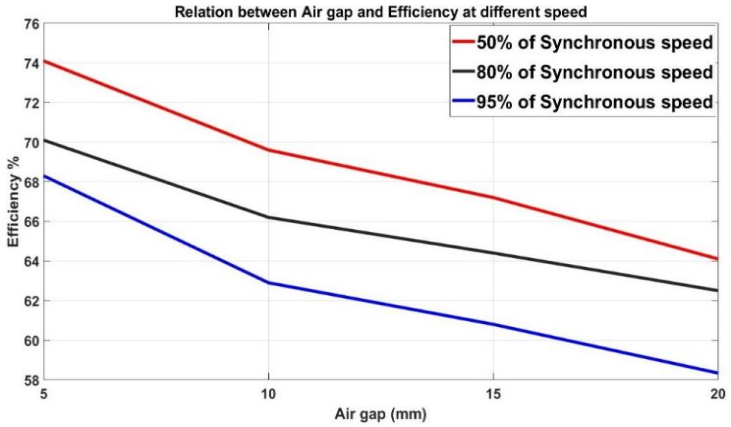

Figure 7. Efficiency versus air gap length characteristic at different speeds

5.1. Analysis and clarification

Calculating the efficiency of a three-phase linear motor depends on the ratio of the output mechanical power (Pout in kW) to the input electrical power (Pin in kW). The efficiency (η) is calculated using the following equation: (η = Pout/Pin×100). The electrical power input to the motor is the total effective power drawn by the motor coils. It is calculated using the equation: $P\text{in} = \sqrt{3} \cdot V\text{L}.\ I\text{L} \cdot \cos(\phi)$ [45]. where VL (line-to-line voltage), (IL) line-to-line current (A), and cos(ϕ) power factor. The mechanical power generated by a linear motor can be calculated as: ($P\text{out} = F \cdot v$). where: F is the mechanical force (Newton) generated by the engine thrust, v is the speed of movement (m/s) [45], [46]. The predicted results show that the optimum value of the air gap must be as small as possible within mechanical limits that prevent contact or friction between moving and stationary parts so as to achieve optimum thrust performance and high efficiency with fewer losses. However, in some cases, reducing the air gap may be more effective up to a certain point, after which it may lead to other problems such as friction or heating. In three-phase linear induction motors, the air gap is usually optimized to obtain the ideal balance between the output thrust power, overall efficiency, and mechanical requirements [47]-[49].

The results of this study have been compared to previous studies. The tendency seen in this study, namely that the thrust force and efficiency drop with increasing length of air gap, is similar to that seen in previous air-gap studies of both single-sided and double-sided LIMs [10]-[12], [36], [37] that report reduction of transmitted thrust force with increasing air gap length due to magnetic leakage and eddy current losses. In the present results, the force variation with air gap is quantified across three operating speeds (Table 2); most

of the studies cited did not report this simultaneously, and the FEM results are compared with an analytical formulation. In summary, Table 2 shows that thrust force falls monotonically as the air gap widens from 5 mm to 30 mm at all three speeds, with the largest relative reduction (about 26%) at the lowest operating speed (24.27 km/h) and the smallest relative reduction (about 13%) at the highest operating speed (48.54 km/h), indicating that the sensitivity of thrust force to air-gap variation is itself speed-dependent, an outcome not simultaneously reported in most of the single-speed studies cited above.

Table 2. Air gap changes with force

Air gap	Force (N) for speed = 24.27 km/h	Force (N) for speed = 38.83 km/h	Force (N) for speed = 48.54 km/h
5 mm	6.633	5.5	4.8
10 mm	5.988	5.1	4.5
15 mm	5.97	5.28	4.6
20 mm	5.3	5	4.5
25 mm	5.1	4.8	4.45
30 mm	4.9	4.7	4.2

5.2. Implications of findings

In addition to the reported thrust and efficiency trends, the fact that leakage flux and eddy-current losses are increasing for higher air gap values is also expected to result in an increase in local heating and a decrease in the dynamic stability margin of the moving part, because a larger and non-uniform air gap will generate non-uniform force distribution across the secondary surface. Although the present FEM electromagnetic study is qualitative, these implications support the practical suggestion that the air gap should be as small as mechanical clearance permits and suggest coupled electromagnetic-thermal-mechanical analysis as an important area for future study. Physically, widening the air gap lowers the mutual magnetic coupling between the primary and secondary because a larger fraction of the primary MMF is consumed in driving flux across the additional reluctance of the air gap itself; this diverts flux into leakage paths instead of the useful working flux that links the secondary sheet, which in turn reduces the induced eddy currents responsible for generating thrust. The associated increase in leakage flux also degrades the uniformity of the traveling-field distribution along the length of the motor, so the electromagnetic force is generated less uniformly across the secondary surface, compounding the loss of net thrust with an increased tendency toward irregular, less stable motion, consistent with the trends reported in Table 2.

These electromagnetic effects also carry direct mechanical and thermal implications for machine reliability. The space harmonics associated with a non-uniform air-gap flux distribution, discussed in section 2, are a recognized source of periodic force ripple, acoustic noise, and vibration, while the additional eddy-current and leakage losses reported above are dissipated as heat within the stator windings and the secondary conductor; a poorly controlled air gap can therefore simultaneously accelerate winding-insulation aging through thermal cycling and increase mechanical wear through sustained vibration. A full quantitative treatment of the resulting harmonic distortion, thermal loading, and electromagnetic interference falls outside the electromagnetic-only scope of the present FEM study and is accordingly highlighted, together with experimental validation, as an important direction for coupled Multiphysics future work.

6. CONCLUSION

A combined analytical and FEM modeling approach is presented in this work. More specifically, the investigation of the effect of the air gap on the operational characteristics of a three-phase linear induction motor (LIM) is studied and focused on. FEM-predicted results are validated with the analytical MMF model and the electromagnetic model and then applied to evaluate the thrust force and efficiency within an air gap range from 5 mm to 30 mm and at three operating speeds. It is worth situating these results relative to conventional rotary induction motors, where the air gap is typically small, fixed, and precisely maintained by bearing tolerances. Because a LIM has no shaft or bearings to constrain the primary-secondary clearance, its air gap is inherently longer and often subject to greater mechanical variability; the air-gap sensitivity trends quantified in this work are therefore of particular practical value for LIM design and are generally more pronounced than the corresponding air-gap effects reported for rotary induction machines.

The results indicate that a higher air gap decreases the coupling magnetic field and the available thrust force, which is increasingly sensitive to the operating speed with increasing air gap size, and that the smallest air gap tested gives the most stable and efficient operation in the range of operating speeds considered. It is found that the air gap between the stator and the moving part, rather than the operating speed, is the most important parameter in order to maximize the thrust force in a three-phase LIM. As the operating speed has a

small effect on the thrust force, while a small air clearance (below 10 mm) should be maintained wherever possible from mechanical considerations, as it improves the thrust force by about 15-35% according to the operating speed based on the force variation. As these figures are derived entirely from analytical and finite-element simulation without experimental corroboration or comparison against an independent published benchmark, they should be interpreted as indicative design trends rather than guaranteed field performance until validated on a physical prototype.

The present conclusions are limited to an electromagnetic FEM analysis and do not include any thermal or mechanical-stability and long-term reliability effects due to air-gap variation, and are valid for the 3.75 kW, 2 pole/7 slot LIM configuration being studied in this work. Future work should include the extension of the present model to consider a coupled electromagnetic-thermal-mechanical analysis, experimental evaluation on a physical prototype for the model predictions, and the investigation of optimized winding and air-gap configurations to improve the efficiency and thrust over a wider range of LIM designs and operating conditions, as well as extending the present steady-state analysis to transient operating regimes such as starting and braking, which are known to impose different and often more severe electromagnetic and thermal demands on the machine than steady-state running. Overall, these results provide a foundation for improving the production methods for LIMs and help to improve their performance and durability for use.

ACKNOWLEDGMENTS

The Authors would like to thank the Department of Electrical Engineering Techniques at Northern Technical University as well as the Department of Electrical Engineering at Mosul University for supporting and encouraging throughout the whole research process.

FUNDING INFORMATION

This research received no external funding.

AUTHOR CONTRIBUTIONS STATEMENT

This journal uses the Contributor Roles Taxonomy (CRediT) to recognize individual author contributions, reduce authorship disputes, and facilitate collaboration.

Name of Author	C	M	So	Va	Fo	I	R	D	O	E	Vi	Su	P
Ahmed Saad Yahya	✓	✓			✓	✓				✓			
Abdullah K. Shanshal	✓	✓		✓		✓			✓	✓			
Ahmed Hasim Ahmed	✓	✓	✓	✓	✓		✓		✓			✓	
Ahmed Jadaan Ali	✓				✓		✓		✓				
Basil Mohammed Saied	✓	✓	✓	✓	✓	✓	✓		✓			✓	
Tamer Kamel	✓	✓				✓	✓			✓			

C : **C**onceptualization
M : **M**ethodology
So : **So**ftware
Va : **Va**lidation
Fo : **Fo**rmal analysis
I : **I**nvestigation
R : **R**esources
D : **D**ata Curation
O : Writing - **O**riginal Draft
E : Writing - Review & **E**diting
Vi : **Vi**sualization
Su : **Su**pervision
P : **P**roject administration

CONFLICT OF INTEREST STATEMENT

The authors declare no conflicts of interest.

DATA AVAILABILITY

The authors confirm that the data supporting the findings of this study are available within the article. Further inquiries can be directed to the corresponding authors.

REFERENCES

[1] T. Sadauskas, A. Smilgevičius, and Z. Savickienė, "Distribution of magnetic field of linear induction motor," *Elektronika ir Elektrotechnika*, vol. 76, no. 4, pp. 63–66, 2007, doi: 10.5755/j02.eie.10721.
[2] S. Yamamura, *Theory of linear induction motors*. Tokyo, Japan: Japan: Tokyo Univ. Press, 1978.

[3] V. Teriaiev, A. Dovbyk, V. Kornienko, M. Pechenik, and S. Buryan, "Generalized mathematical model of a linear induction motor," *Proceedings - IEEE International Conference on Electronics and Nanotechnology, ELNANO*, pp. 741–745, 2022, doi: 10.1109/ELNANO54667.2022.9927095.
[4] N. El Ouanjli, S. Motahhir, A. Derouich, A. El Ghzizal, A. Chebabhi, and M. Taoussi, "Improved dtc strategy of doubly fed induction motor using fuzzy logic controller," *Energy Reports*, vol. 5, pp. 271–279, 2019, doi: 10.1016/j.egyr.2019.02.001.
[5] J. A. Toledo, L. A. R. Silva and T. A. C. Maia, "Modeling of three-phase induction machines under combined inter-turn fault and mechanical eccentricity," in IEEE Access, vol. 13, pp. 178478-178491, 2025, doi: 10.1109/ACCESS.2025.3621153.
[6] T. Zhou, Y. Du, J. Han and W. Xu, "Performance analysis of a linear induction motor based on the finite element method," *2009 International Conference on Applied Superconductivity and Electromagnetic Devices*, Chengdu, China, 2009, pp. 163-166, doi: 10.1109/ASEMD.2009.5306666.
[7] F. N. Sarapulov, V. E. Frizen, E. L. Shvydkiy, and I. A. Smol'yanov, "Mathematical modeling of a linear-induction motor based on detailed equivalent circuits," *Russian Electrical Engineering*, vol. 89, no. 4, pp. 270–274, 2018, doi: 10.3103/S1068371218040119.
[8] R. M. Pai, I. Boldea, and S. A. Nasar, "Complete equivalent circuit of a linear induction motor with sheet secondary.," *IEEE Transactions on Magnetics*, vol. 24, no. 1, pp. 639–654, 1987, doi: 10.1109/20.43997.
[9] Gundugdu, Tayfun; Komurgoz, Guven./Design of permanent magnet machines with different rotor type. In: World Academy of Science, Engineering and Technology. 2010; Hac. 46. pp. 510-515.
[10] M. S. Manna, S. Marwaha, and N. Kaur, "Air gap field analysis of single sided linear induction motor with time harmonic finite element method," in *Proceedings of the COMSOL Conference 2010 India*, 2010, pp. 2–5.
[11] J. Lu and W. Ma, "Dynamic characteristic analysis of high speed long primary block feeding linear induction motor," in *Proceedings of the 11th International Conference on Electrical Machines and Systems, ICEMS 2008*, 2008, pp. 3459–3463.
[12] D. H. Im and C. E. Kim, "Finite element force calculation of a linear induction motor taking account of the movement," *IEEE Transactions on Magnetics*, vol. 30, no. 5, pp. 3495–3498, 1994, doi: 10.1109/20.312692.
[13] A. S. Ghodake and U. Patil, "Experimental analysis of field oriented control technique for three-phase induction motor drive in electric vehicles application," *2024 2nd International Conference on Advancements and Key Challenges in Green Energy and Computing (AKGEC)*, Ghaziabad, India, 2024, pp. 1-4, doi: 10.1109/AKGEC62572.2024.10868658.
[14] D. R. Gomes and I. E. Chabu, "A novel analytical equivalent circuit for single-sided linear induction motors considering secondary leakage reactance," *Energies*, vol. 16, no. 3, 2023, doi: 10.3390/en16031261.
[15] F. Lftisi, G. H. George, and M. A. Rahman, "Implementing fuzzy logic controller techniques for indirect vector control induction motor drives," *2017 8th IEEE Annual Information Technology, Electronics and Mobile Communication Conference, IEMCON 2017*, pp. 6–11, 2017, doi: 10.1109/IEMCON.2017.8117129.
[16] S. H. Im and B. G. Gu, "Study of induction motor inter-turn fault part I: development of fault models with distorted flux representation," *Energies*, vol. 15, no. 3, 2022, doi: 10.3390/en15030894.
[17] G. Lv, S. Yan, D. Zeng, and T. Zhou, "An equivalent circuit of the single-sided linear induction motor considering the discontinuous secondary," *IET Electric Power Applications*, vol. 13, no. 1, pp. 31–37, 2019, doi: 10.1049/iet-epa.2018.5184.
[18] H. H. Chiang, K. C. Hsu, and I. H. Li, "Optimized adaptive motion control through an sopc implementation for linear induction motor drives," *IEEE/ASME Transactions on Mechatronics*, vol. 20, no. 1, pp. 348–360, 2015, doi: 10.1109/TMECH.2014.2313594.
[19] M. N. Raju and M. S. Rani, "Mathematical modelling of linear induction motor," *International Journal of Engineering and Technology*, vol. 7, no. 4.24, pp. 111–114, 2018, doi: 10.14419/ijet.v7i4.24.21868.
[20] H. Hamzehbahmani, "Investigation of dynamic performance of short rotor linear induction motor while fed by different types of voltage source inverters," in *Proc. 16th Iranian Conf. Electrical Engineering (ICEE2008)*, 2008, pp. 248–253.
[21] M. S. Manna, S. Marwaha, and A. Marwaha, "Computation & analysis of end region em force for electrical rotating machines using fem," in *2006 International Conference on Power Electronic, Drives and Energy Systems*, IEEE, Dec. 2006, pp. 1–5, doi: 10.1109/PEDES.2006.344297.
[22] Xuhui Wen, Ruoping Yao, and J. A. Tegopoulos, "Transient quasi-3d method in the transient electromagnetic field calculation of end region of turbo-generator," *IEEE Transactions on Magnetics*, vol. 30, no. 5, pp. 3709–3712, Sep. 1994, doi: 10.1109/20.312747.
[23] A. Z. Bazghaleh, M. R. Naghashan, M. R. Meshkatoddini, and H. Mahmoudimanesh, "Optimum design of high speed single-sided linear induction motor to obtain best performance," in *SPEEDAM 2010*, IEEE, Jun. 2010, pp. 1222–1226, doi: 10.1109/SPEEDAM.2010.5545154.
[24] A. Kushwaha and M. Gopal, "Fuzzy logic controller performance in vector control of induction machine," in *Proceedings of 2017 IEEE International Conference on Technological Advancements in Power and Energy: Exploring Energy Solutions for an Intelligent Power Grid, TAP Energy 2017*, 2018, pp. 1–5, doi: 10.1109/TAPENERGY.2017.8397343.
[25] L. S. Maraaba, A. S. Milhem, I. A. Nemer, H. Al-Duwaish, and M. A. Abido, "Convolutional neural network-based inter-turn fault diagnosis in lspmsms," *IEEE Access*, vol. 8, pp. 81960–81970, 2020, doi: 10.1109/ACCESS.2020.2991137.
[26] G. Singh and G. Singh, "Modeling and simulation of indirect field oriented control of three phase induction motor using fuzzy logic controller," vol. 3, no. 8, pp. 1126–1131, 2014.
[27] N. J. Merlin Mary, C. Ganguly, and M. Kowsalya, "Mathematical modelling of linear induction motor with and without considering end effects using different reference frames," *1st IEEE International Conference on Power Electronics, Intelligent Control and Energy Systems, ICPEICES 2016*, 2017, doi: 10.1109/ICPEICES.2016.7853160.
[28] A. H. Ahmed, A. S. Yahya, and A. J. Ali, "Speed control for linear induction motor based on intelligent pi-fuzzy logic," *Journal of Robotics and Control (JRC)*, vol. 5, no. 5, pp. 1470–1478, 2024, doi: 10.18196/jrc.v5i5.22203.
[29] W. Ma, L. Xi, Y. Zhang, Z. He, X. Zhang, and Z. Cai, "Design and comparison of linear induction motor and superconducting linear synchronous motor for electromagnetic launch," *2021 13th International Symposium on Linear Drives for Industry Applications, LDIA 2021*, 2021, doi: 10.1109/LDIA49489.2021.9505785.
[30] Z. Sun, L. Xu, W. Zhao, and K. Du, "Comparison between linear induction motor and linear primary permanent magnet vernier motor for railway transportation," *2021 13th International Symposium on Linear Drives for Industry Applications, LDIA 2021*, 2021, doi: 10.1109/LDIA49489.2021.9505835.
[31] Z. Jiang *et al.*, "Structural optimization of linear induction motor for reducing end effect," *2020 IEEE 9th International Power Electronics and Motion Control Conference, IPEMC 2020 ECCE Asia*, pp. 1998–2001, 2020, doi: 10.1109/IPEMC-ECCEAsia48364.2020.9367699.
[32] K. Sannomiya, T. Morizane, N. Kimura, and H. Omori, "Experimental confirmation of thrust and attractive force control for linear induction motor by two different frequency components," *LDIA 2017 - 11th International Symposium on Linear Drives for Industry Applications*, 2017, doi: 10.23919/LDIA.2017.8097260.

[33] E. Amiri, "Study of linear induction motor end effects using 3-d fem and equivalent circuit," *IECON Proceedings (Industrial Electronics Conference)*, pp. 3165–3170, 2013, doi: 10.1109/IECON.2013.6699634.
[34] H.-W. Lee, C.-B. Park, and B.-S. Lee, "Thrust performance improvement of a linear induction motor," *Journal of Electrical Engineering and Technology*, vol. 6, no. 1, pp. 81–85, 2011, doi: 10.5370/jeet.2011.6.1.081.
[35] S. Il Kim, J. P. Hong, Y. K. Kim, H. Nam, and H. I. Cho, "Optimal design of slotless-type pmlsm considering multiple responses by response surface methodology," *IEEE Transactions on Magnetics*, vol. 42, no. 4, pp. 1219–1222, 2006, doi: 10.1109/TMAG.2006.871950.
[36] G. Kong, L. Shi, J. Liu, S. Zhou, X. Cao, and Y. Li, "Discrete resonant controller based current harmonics suppression for dual three-phase linear induction motor," *2023 14th International Symposium on Linear Drivers for Industry Applications, LDIA 2023*, 2023, doi: 10.1109/LDIA59564.2023.10297476.
[37] A. Z. Bazghaleh, M. R. Naghashan, and M. R. Meshkatoddini, "Optimum design of single-sided linear induction motors for improved motor performance," *IEEE Transactions on Magnetics*, vol. 46, no. 11, pp. 3939–3947, 2010, doi: 10.1109/TMAG.2010.2062528.
[38] A. Bensehila, A. Bouzidi, and N. Takorabet, "Space harmonics effects on performances of linear induction motors: modelization and characterization," *Actuators*, vol. 12, no. 12, 2023, doi: 10.3390/act12120440.
[39] B. J. Lee, D. H. Koo, and Y. H. Cho, "Investigation of linear induction motor according to secondary conductor structure," *IEEE Transactions on Magnetics*, vol. 45, no. 6, pp. 2839–2842, 2009, doi: 10.1109/TMAG.2009.2018687.
[40] A. M. Tavares, A. F. F. Filho, and D. G. Dorrell, "A variable parameter three-phase model for a linear induction machine operating in regenerative brake mode," *Proceedings: IECON 2018 - 44th Annual Conference of the IEEE Industrial Electronics Society*, pp. 361–366, 2018, doi: 10.1109/IECON.2018.8591474.
[41] H. Hamzehbahmani, "Modeling and simulating of single side short stator linear induction motor with the end effect," *Journal of Electrical Engineering*, vol. 62, no. 5, pp. 302–308, 2011, doi: 10.2478/v10187-011-0048-5.
[42] J. Lu and W. Ma, "Research on end effect of linear induction machine for high-speed industrial transportation," *IEEE Transactions on Plasma Science*, vol. 39, no. 1 PART 1, pp. 116–120, 2011, doi: 10.1109/TPS.2010.2085089.
[43] L. Zhang, H. Obeid, S. Laghrouche, and M. Cirrincione, "Second order sliding mode observer of linear induction motor," *IET Electric Power Applications*, vol. 13, no. 1, pp. 38–47, 2019, doi: 10.1049/iet-epa.2018.5232.
[44] H. Hirahara, M. Inoue, and S. Yamamoto, "A method for determining equivalent circuit constant of linear induction motors using locked mover and standstill impedance tests," *2022 International Power Electronics Conference, IPEC-Himeji 2022-ECCE Asia*, pp. 807–812, 2022, doi: 10.23919/IPEC-Himeji2022-ECCE53331.2022.9806981.
[45] V. Teriaiev, A. Dovbyk, V. Kornienko, M. Pechenik, and S. Buryan, "Generalized mathematical model of a linear induction motor," in *Proceedings - IEEE International Conference on Electronics and Nanotechnology, ELNANO*, 2022, pp. 741–745, doi: 10.1109/ELNANO54667.2022.9927095.
[46] A. H. Isfahani, B. M. Ebrahimi, and H. Lesani, "Design optimization of a low-speed single-sided linear induction motor for improved efficiency and power factor," *IEEE Transactions on Magnetics*, vol. 44, no. 2, pp. 266–272, 2008, doi: 10.1109/tmag.2007.912646.
[47] R. A. H. De Oliveira, D. Berger, L. Schultz, R. M. Stephan, and A. C. Ferreira, "Finite element analysis of the forces developed on linear induction motors," *2015 IEEE 13th Brazilian Power Electronics Conference and 1st Southern Power Electronics Conference, COBEP/SPEC 2016*, 2015, doi: 10.1109/COBEP.2015.7420063.
[48] S. C. Park and B. T. Kim, "Effect of contact resistance between side-bar and secondary conductors in a linear induction motor with a cage-type secondary," *IEEE Transactions on Magnetics*, vol. 39, no. 3 I, pp. 1562–1565, 2003, doi: 10.1109/TMAG.2003.810341.
[49] G. Lv, D. Zeng, T. Zhou, and M. Degano, "A complete equivalent circuit for linear induction motors with laterally asymmetric secondary for urban railway transit," *IEEE Transactions on Energy Conversion*, vol. 36, no. 2, pp. 1014–1022, 2021, doi: 10.1109/TEC.2020.3026334.

BIOGRAPHIES OF AUTHORS



Ahmed Saad Yahya is a lecturer in the Department of Electrical Engineering Techniques at the Engineering Technical College, Mosul, Iraq. He received his B.Sc. and M.Sc. degrees in electrical engineering from the University of Mosul, Iraq, in 2012 and 2017, respectively. His research interests include adaptive and intelligent control systems, electric machine design, and electric drives. He can be contacted at email: ahmed.saad.yahya@ntu.edu.iq.



Abdullah K. Shanshal received his Bachelor of Technology (B.Tech.) degree in electrical power technology engineering from the Engineering Technical College, Northern Technical University, Mosul, Iraq, in 2005, and his Master of Technology (M.Tech.) degree in the same field from the same institution in 2010. He received his Ph.D. in electrical engineering from the University of Sheffield, Sheffield, United Kingdom, in 2019. His research interests include the design and investigation of novel permanent-magnet electric machines with high torque and power density, high efficiency, low cost, and high performance for various applications, including electric and hybrid vehicles and domestic appliances. He can be contacted at email: a.shanshal@ntu.edu.iq.



Ahmed Hasim Ahmed is a lecturer at the Engineering Technical College for Computer and Artificial Intelligence, Mosul, Iraq. He received his B.Sc. and M.Sc. degrees in electrical engineering from the University of Mosul, Iraq, in 2011 and 2014, respectively. His research interests include adaptive and intelligent control systems, electric machine design, and electric drives. He can be contacted at email: ahmed.h.ahmed@ntu.edu.iq.



Ahmed Jadaan Ali is a lecturer in the Department of Electrical Power Engineering Technology at the Engineering Technical College, Mosul, Iraq. He received his B.Sc. and M.Sc. degrees in electrical engineering from the University of Technology, Baghdad, Iraq, in 1995 and 2004, respectively. He received his Ph.D. in electrical machines from the University of Mosul, Iraq, in 2012. During his Ph.D. studies, he undertook a six-month research scholarship at the University of the Bundeswehr Munich, Germany. His research interests include adaptive and intelligent control systems, electric machine design, and electric drives. He can be contacted at email: ahmed.j.ali@ntu.edu.iq.



Basil Mohammed Saied is currently a professor emeritus of power electronics in the Department of Electrical Engineering at the University of Mosul, Iraq. He received his Doctor of Philosophy degree from the University of Bath, United Kingdom, in 1983; his Master of Science degree from the University of Bradford, United Kingdom, in 1980; and his Bachelor of Science degree from the University of Mosul, Iraq, in 1977. His main research interests include power electronics and electrical machines. He can be contacted at email: bmsaied@gmail.com.



Tamer Kamel received his Bachelor of Science and Master of Science degrees in electrical engineering from Cairo University, Giza, Egypt, in 2007 and 2010, respectively, and his Doctor of Philosophy degree in electrical power engineering from the University of New Brunswick, Fredericton, Canada, in 2015. He is currently a lecturer in power electronics and renewable energy at the School of Engineering, Computing, and Mathematics, University of Plymouth, United Kingdom. He leads several projects on renewable energy integration, electrified transport, and maritime decarbonization. He has published and presented more than 40 articles and papers in high-ranking international journals and conference proceedings. He is also an associate member of the Institute of Marine Engineering, Science and Technology and a Fellow of the Higher Education Academy. He can be contacted at email: tamer.kamel@plymouth.ac.uk.